ELSEVIER

Journal of Alloys and Compounds 432 (2007) 232–240

Journal of ALLOYS AND COMPOUNDS

www.elsevier.com/locate/jallcom

# Phase transitions in $[Ca(H_2O)_4](NO_3)_2$ studied by differential scanning calorimetry, X-ray single crystal diffraction and neutron powder diffraction: Part I

Anna Migdał-Mikuli [a], Joanna Hetmańczyk [a], Wojciech Nitek [b], Edward Mikuli [a], Łukasz Hetmańczyk [a,*]

[a] *Department of Chemical Physics, Faculty of Chemistry, Jagiellonian University, ul. Ingardena 3, 30-060 Kraków, Poland*
[b] *Department of Crystal Chemistry and Crystal Physics, Faculty of Chemistry, Jagiellonian University, ul. Ingardena 3, 30-060 Kraków, Poland*

Received 10 April 2006; accepted 28 May 2006
Available online 7 July 2006

**Abstract**

Two phase transitions at: $T_{C1}^{h} = 243.7$ K and $T_{C2}^{h} = 203.3$ K (on heating) and at: $T_{C1}^{c} = 222.0$ K and $T_{C2}^{c} = 201.5$ K (on cooling) were determined for $[Ca(H_2O)_4](NO_3)_2$ between 90 and 300 K by means of differential scanning calorimetry (DSC). Large thermal hysteresis (~22 K) of $T_{C1}$ phase transition is characteristic for similar compounds indicating high degree of dynamical disorder of $NO_3^-$ anions. Phase transition discovered at $T_{C2}$ is connected with small change of the crystal structure. Namely, at low temperature phase the unit cell is doubled and there are scant but statistically significant differences between atom positions at 100 and 215 K. The space group ($P2_1/n$; No. 14) is the same for high, intermediate and low temperature phase, however, changes of water molecules orientations and changes in the net of hydrogen bonds are distinctly visible.


*Keywords:* Tetraaquacalcium nitrate(V); Phase transitions; Structural changes; Differential scanning calorimetry; X-ray single crystal diffraction; Neutron powder diffraction

## 1. Introduction

The crystal lattice parameters of tetraaquacalcium nitrate(V) crystal structure were determined at room temperature (RT) by Leclaire and Monier [1,2] and also by Ribar and Divjaković [3]. The title compound crystallizes in monoclinic crystal system in the space group No. $14 = P2_1/n$. The crystal structure contains $[Ca_2(H_2O)_8](NO_3)_4$ dimers, joined by hydrogen bonds [1–3]. There are two crystallographically non-equivalent, slightly distorted, $NO_3^-$ ions. We have performed X-ray measurements for the single crystal at RT in order, among others, to check the proper composition of investigated by us compound. Crystal lattice parameters obtained by us and their comparison with the literature data were presented in Table 1. The data obtained in this work are very similar to those obtained earlier [3].

The polymorphism of crystalline compounds of the type $[M(H_2O)_6](NO_3)_2$ is only up to now known for M = Mg, Mn, Co, Ni, Cu and Zn [4–6]. All of these compounds exhibited two stage melting process. However, only two of them, namely: $[Co(H_2O)_6](NO_3)_2$ and $[Mg(H_2O)_6](NO_3)_2$, indicated at the temperature range of 100–400 K one solid–solid phase transition [4,5].

The main aim of this paper is to investigate the polymorphism of the titled compound and to find its connection with the changes in the crystal structure. Unfortunately, the crystal structures of both: the low and intermediate temperature phase were up to now unknown. Thus, one of the aims of this paper is also to determine a crystal structure of these both phases. In our next paper (Part II) we would like to find some connection of the detected phase transitions with the orientational dynamic of molecular groups: $H_2O$ and $NO_3^-$ by means of Raman and infrared spectroscopy and by nuclear magnetic resonance method.

## 2. Experimental procedures

$[Ca(H_2O)_4](NO_3)_2$ was synthesized by treating calcium carbonate with diluted nitric acid. The solution was concentrated by mild heating, and

* Corresponding author. Fax: +48 12 634 0515.
*E-mail address:* hetmancz@chemia.uj.edu.pl (Ł. Hetmańczyk).

0925-8388/$ – see front matter © 2006 Elsevier B.V. All rights reserved.
doi:10.1016/j.jallcom.2006.05.128

Table 1
Crystal data for $[Ca(H_2O)_4](NO_3)_2$ at room temperature

| | This work ($P2_1/n$)[a] | [3] ($P2_1/n$)[a] | [1] ($P2_1/n$)[a] | [2] ($P2_1/n$)[a] |
|---|---|---|---|---|
| $a$ (Å) | 6.282(2) | 6.277(7) | 6.268(6) | 6.2786(7) |
| $b$ (Å) | 9.156(6) | 9.157(9) | 9.116(9) | 9.1551(5) |
| $c$ (Å) | 14.475(1) | 14.484(10) | 14.830(10) | 14.8999(12) |
| $\beta$ (°) | 98.3(9) | 98.6(2) | 106.5(3) | 106.22(1) |
| $Z$ | 4 | 4 | 4 | 4 |

[a] Space group.

colourless crystals obtained after cooling the solution were purified several times by repeated crystallization from four-time distilled water. Then, the crystals were dried for several days in a desiccator over BaO and stored in hygrostat. The composition of the compound was established through chemical and thermal analysis [7].

DSC measurements at 95–300 K were performed with a Perkin-Elmer PYRIS 1 DSC apparatus. The samples of masses: 19.49 and 17.54 mg were placed in an aluminium vessel and closed by compressing. Another empty aluminium vessel was used as a reference holder. Two characteristic temperatures of the DSC peaks obtained on heating and on cooling the sample were computed: temperature of the peak maximum ($T_{peak}$) and temperature calculated from a slope of the left-hand side (on heating) or the right-hand side (on cooling) of the peak ($T_{onset}$). These two temperatures differed by 2–4 K, what depended on the scanning rate of heating or cooling. The enthalpy change ($\Delta H$) was calculated by numerical integration of the DSC curve under the anomaly peak after a linear background arbitrary subtraction. The entropy change ($\Delta S$) was calculated using the formula $\Delta S = \Delta H/T_C$. For sharp peaks the values were calculated to a high accuracy (4%), whereas for the diffuse peak they were estimated only. Other experimental details were the same as those published in our previous paper [8].

X-ray diffraction intensity measurements performed for single crystal sample at 293, 215 and 100 K were carried out on a Nonius Kappa CCD diffractometer equipped with molybdenum X-ray tube and Oxford Cryostream cooler. The same data collection strategy (complete sphere of reciprocal space, 6 s exposure time) was used for each of these three experiments. Collected data were processed using DENZO-SCALEPACK [9]. The phase problem was solved using SIR-92 program [10] and the refinement was performed with SHELXL-97 [11]. Positions of the hydrogen atoms were located from the difference Fourier maps and refined positionally with individual isotropic thermal parameters. The hydrogen atoms were refined with geometrical (bond length) restrains only for 293 and 215 K. All non-H atoms were refined anisotropically. Details of the measurement and refinement are given in Table 2.

Neutron powder diffraction (NPD) patterns were measured simultaneously with incoherent, inelastic/quasielastic neutron scattering (IINS/QENS) spectra using the time-of-flight method in the NERA-PR spectrometer [12] in the high flux pulsed reactor IBR-2, at Dubna (Russia). The sample was put into a thin-wall aluminium container (140 mm × 60 mm × 1 mm) at room temperature. The sample holder was then placed in a top-loaded cryostat cooled with a helium refrigerator. The temperature of the sample could be changed within the range 20–300 K and stabilized with ±0.5 K accuracy at any chosen value. In the case of the NPD, different scattering angles were used to record the selected lattice spacing $d_{hkl}$ ranges at an appropriate resolution. It should be emphasized that, because the examined compound contained ca. 50% of hydrogen atoms, the NPD patterns were recorded against a relatively high incoherent background due to incoherent scattering of hydrogen atoms. For this reason, their interpretation is only qualitative, nevertheless it was very useful for identification of particular phases.

## 3. Results and discussion

### 3.1. DSC measurements

The DSC measurements were performed both on heating and cooling a sample with a mass equal to 19.49 mg (sample I) and the second sample with a mass equal to 17.54 mg (sample II), at constant rates of 10, 20, 30 and 40 K $min^{-1}$.

Table 2
Experimental details and results of X-ray diffraction experiments

| | Temperature (K) | | |
|---|---|---|---|
| | 293.0(2) | 215.0(1) | 100.0(1) |
| Empirical formula | $Ca(NO_3)\cdot 4H_2O$ | $Ca(NO_3)\cdot 4H_2O$ | $Ca(NO_3)\cdot 4H_2O$ |
| Formula weight | 236.16 | 236.16 | 236.16 |
| Wavelength | 0.71073 Å | 0.71073 Å | 0.71073 Å |
| Crystal system, space group | Monoclinic, $P2_1/n$ | Monoclinic, $P2_1/n$ | Monoclinic, $P2_1/n$ |
| Unit cell dimensions | $a = 6.282(5)$ Å, $b = 9.157(5)$ Å, $c = 14.475(5)$ Å, $\beta = 98.386(5)^\circ$ | $a = 6.235(5)$ Å, $b = 9.146(5)$ Å, $c = 14.406(5)$ Å, $\beta = 98.285(5)^\circ$ | $a = 12.423(5)$ Å, $b = 9.120(5)$ Å, $c = 14.727(5)$ Å, $\beta = 105.748(5)^\circ$ |
| Volume | 823.8(8) $Å^3$ | 812.9(8) $Å^3$ | 1605.9(12) $Å^3$ |
| $Z$ | 4 | 4 | 8 |
| Density (calculated) | 1.904 $mg/m^3$ | 1.930 $mg/m^3$ | 1.954 $mg/m^3$ |
| Absorption coefficient | 0.806 $mm^{-1}$ | 0.816 $mm^{-1}$ | 0.827 $mm^{-1}$ |
| $F(0\,0\,0)$ | 488 | 488 | 976 |
| Crystal size | 0.6 mm × 0.55 mm × 0.5 mm | 0.6 mm × 0.55 mm × 0.5 mm | 0.6 mm × 0.55 mm × 0.5 mm |
| Theta range for data collection | 3.38–27.48° | 2.65–27.47° | 2.81–27.49° |
| Index ranges | $-8 \le h \le 8$, $-11 \le k \le 11$, $-18 \le l \le 18$ | $-8 \le h \le 8$, $-8 \le k \le 11$, $-18 \le l \le 18$ | $-16 \le h < \le 16$, $-11 \le k \le 11$, $-19 \le l \le 18$ |
| Reflections collected | 3635 | 3581 | 7115 |
| Independent reflections | 1888 [$R$(int) = 0.0000] | 1850 [$R$(int) = 0.0086] | 3675 [$R$(int) = 0.0098] |
| Completeness to theta = 27.48° | 99.8% | 99.9% | 99.8% |
| Refinement method | Full-matrix least-squares on $F^2$ | Full-matrix least-squares on $F^2$ | Full-matrix least-squares on $F^2$ |
| Data/restraints/parameters | 1880/8/151 | 1851/8/151 | 3675/0/300 |
| Goodness-of-fit on $F^2$ | 1.112 | 1.096 | 1.094 |
| Final $R$ indices [$I > 2$sigma($I$)] | $R1 = 0.0220$, $wR2 = 0.0570$ | $R1 = 0.0201$, $wR2 = 0.0539$ | $R1 = 0.0199$, $wR2 = 0.0532$ |
| $R$ indices (all data) | $R1 = 0.0244$, $wR2 = 0.0585$ | $R1 = 0.0219$, $wR2 = 0.0553$ | $R1 = 0.0247$, $wR2 = 0.0558$ |
| Extinction coefficient | 0.064 (3) | 0.034 (2) | 0.0055 (4) |
| Largest diff. peak and hole | 0.276 and −0.224 e $Å^{-3}$ | 0.271 and −0.226 e $Å^{-3}$ | 0.213 and −0.294 e $Å^{-3}$ |

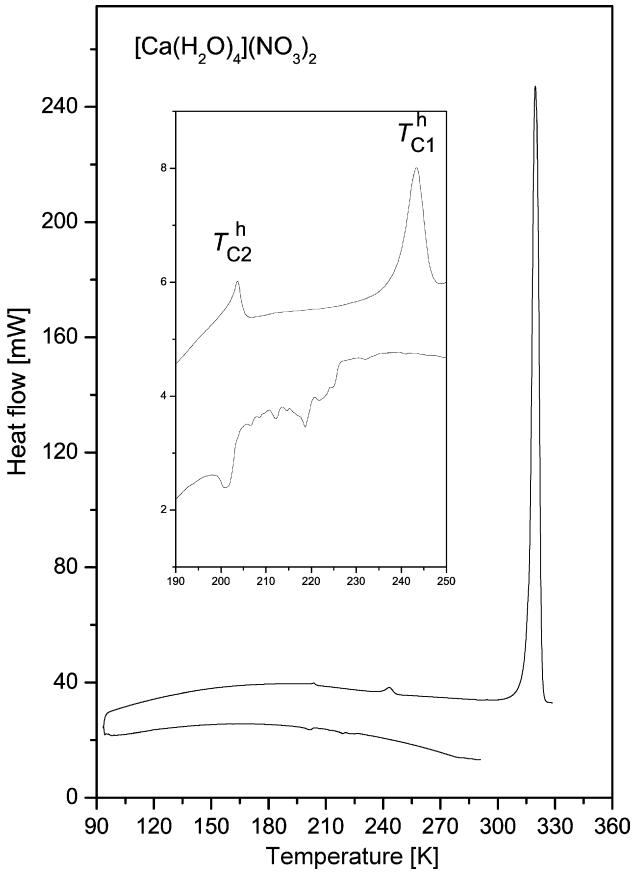


Fig. 1. DSC curves registered on first cooling and heating of $[Ca(H_2O)_4](NO_3)_2$ (sample I) at a scanning rate of 20 K min$^{-1}$ in the temperature range of 90–330 K.

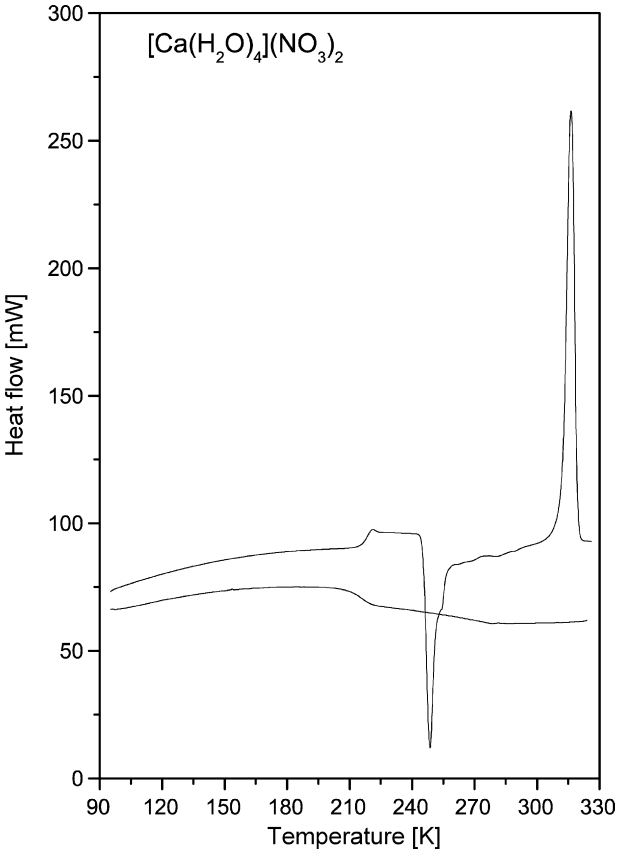


Fig. 2. DSC curves registered on cooling of melted sample I of $[Ca(H_2O)_4](NO_3)_2$ and subsequent heating at a rate of 20 K min$^{-1}$ in the temperature range of 90–330 K.

Sample I was measured in the temperature range of 90–330 K in order to investigate melting process of the title compound. Fig. 1 shows the temperature dependences of the heat flow (DSC curves) obtained while first cooling (lower curve) and subsequent heating (upper curve) of $[Ca(H_2O)_4](NO_3)_2$ sample I at the rate of 20 K min$^{-1}$. In Fig. 1 one can see three anomalies on the upper curve (heating curve). Two of them at $T^h_{C1}$ and $T^h_{C2}$ are very small in comparison with the third one which is connected with the melting of the sample at $T_m = 317.6$ K. These small anomalies are better visible in the insertion, also presented in Fig. 1. While cooling the liquid (melted or rather better to say dissolved in own coordinated water) sample I from 330 to 90 K at a rate of 20 K min$^{-1}$, only characteristic glass transition on the DSC curve at ca. 215 K was recorded, as can be seen in Fig. 2. Thus a metastable glass phase was formed. Next heating of this glass sample from 90 to 330 K, first at ca. 215 K glass transition take place and next a re-crystallization into a crystalline phase as an exothermic sharp peak at ca. 247 K can be observed. Subsequent heating lead to melting of the crystal at ca. 318 K.

Sample II was measured in the temperature range of 90–295 K in order to careful investigation of the phase transitions in solid state at $T_{C1}$ and $T_{C2}$. Fig. 3 presents the temperature dependences of the heat flow obtained for the title compound on heating (upper curve) and on cooling (down curve) sample II of $[Ca(H_2O)_4](NO_3)_2$ at the rate of 20 K min$^{-1}$. Two distinct anomalies were registered on each of these two DSC curves at: $T^h_{C1\,peak} = 244.1$ K and $T^h_{C2\,peak} = 203.5$ K (on heating) and at $T^c_{C1\,peak} = 221.9$ K and $T^c_{C2\,peak} = 201.2$ K (on cooling). The phase transitions temperatures: $T^h_{C1} = 243.7$ K and $T^h_{C2} = 203.3$ K (on heating) and at $T^c_{C1} = 222.0$ K and $T^c_{C2} = 201.5$ K (on cooling) were calculated by extrapolating the corresponding dependencies of $T^h_{peak}$ and $T^c_{peak}$ values versus the scanning rate dependences, registered at four scanning rates of heating and cooling the sample: 10, 20, 30 and 40 K min$^{-1}$, to the scanning rate value equal to 0 K min$^{-1}$. The presence of ca. 20 K hysteresis of the phase transition temperature at $T_{C1}$ and the heat flow anomaly sharpness suggest that the detected phase transition is a first-order one. The second phase transition at $T_{C2}$ is probably connected with the second order phase transition. It is also suggested by the "lambda shape" of the anomaly. The thermodynamic parameters of the detected phase transitions are presented in Table 3.

### 3.2. X-ray diffraction

Table 2 presents experimental details of X-ray measurement of single crystalline sample of $[Ca(H_2O)_4](NO_3)_2$. Contents of the asymmetric unit of the unit cell of $[Ca(H_2O)_4](NO_3)_2$ crystal at room temperature (293 K) is consistent with empirical formula. Each $Ca^{2+}$ cation coordinates four $H_2O$ molecules with mean $Ca^{2+}$–O distance equals to 2.443 Å and five oxygen atoms

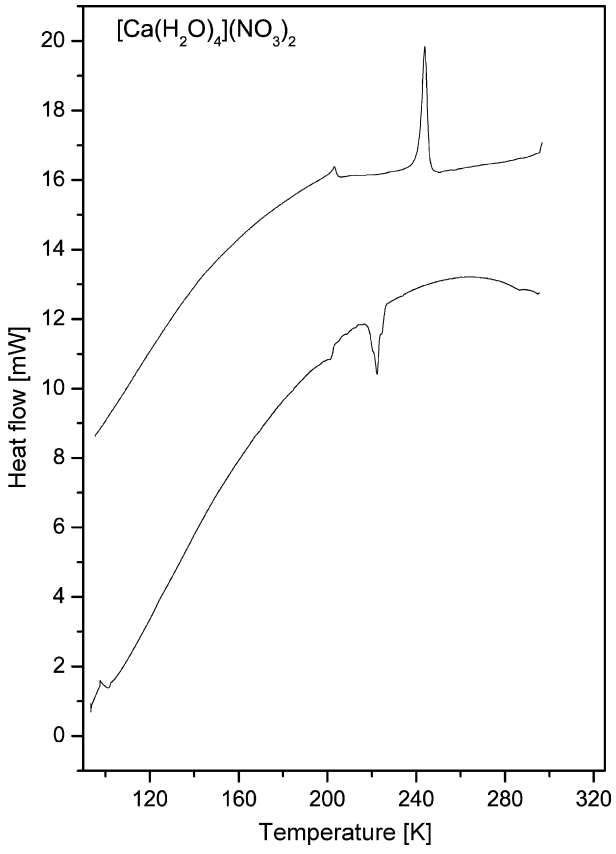


Fig. 3. DSC curves registered on heating and cooling of $[Ca(H_2O)_4](NO_3)_2$ (sample II) at a rate of 20 K min$^{-1}$ in the temperature range of 90–295 K.

Table 3
Thermodynamic parameters of the phase transitions of $[Ca(H_2O)_4](NO_3)_2$

| Parameters | Heating | Cooling |
|---|---|---|
| $T_m$ (K) | 317.6 ± 0.1 | |
| $T_{C1}$ (K) | 243.7 ± 0.1 | 222.0 ± 0.1 |
| $T_{C2}$ (K) | 203.3 ± 0.1 | 201.5 ± 0.1 |
| $\Delta H_m$ (kJ mol$^{-1}$) | 34.28 ± 1.57 | |
| $\Delta H_1$ (kJ mol$^{-1}$) | 1.41 ± 0.20 | 0.86 ± 0.03 |
| $\Delta H_2$ (kJ mol$^{-1}$) | 0.16 ± 0.01 | 0.15 ± 0.01 |
| $\Delta S_m$ (J mol$^{-1}$ K$^{-1}$) | 107.9 ± 4.3 | |
| $\Delta S_1$ (J mol$^{-1}$ K$^{-1}$) | 5.8 ± 0.4 | 3.9 ± 0.2 |
| $\Delta S_2$ (J mol$^{-1}$ K$^{-1}$) | 0.8 ± 0.01 | 0.7 ± 0.01 |

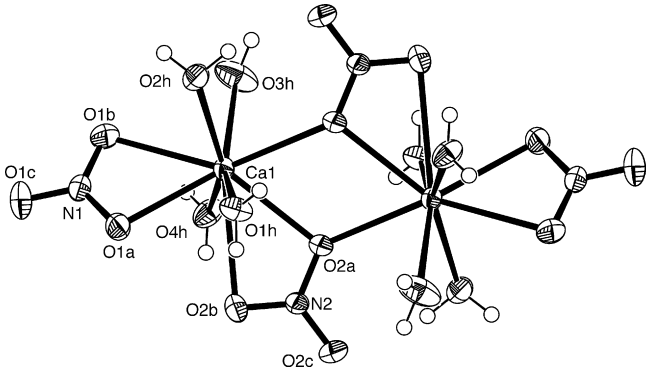


Fig. 4. ORTEP [13,14] projections of the molecular structure of the $[Ca(H_2O)_4](NO_3)_2$ dimer at RT.

Table 4
Atomic coordinates ($10^{-4}$) and equivalent isotropic displacement parameters ($\times 10^3$ Å$^2$) for the structures of the $[Ca(H_2O)_4](NO_3)_2$ determined at temperatures: 293, 215 and 100 K

| | $x$ | $y$ | $z$ | $U$(eq) |
|---|---|---|---|---|
| 293 K | | | | |
| Ca(1) | 5394(1) | 4103(1) | 3671(1) | 21(1) |
| N(1) | 5980(2) | 3720(1) | 1693(1) | 26(1) |
| N(2) | 4264(2) | 7329(1) | 4067(1) | 23(1) |
| O(1a) | 6601(2) | 4838(1) | 2169(1) | 37(1) |
| O(1b) | 5252(2) | 2685(1) | 2119(1) | 36(1) |
| O(1c) | 6109(2) | 3654(1) | 857(1) | 43(1) |
| O(2a) | 4184(2) | 6212(1) | 4586(1) | 31(1) |
| O(2b) | 4770(2) | 7124(1) | 3277(1) | 31(1) |
| O(2c) | 3850(2) | 8548(1) | 4347(1) | 39(1) |
| O(2h) | 8172(2) | 2225(1) | 3968(1) | 39(1) |
| O(3h) | 3106(2) | 1970(2) | 3855(1) | 54(1) |
| O(1h) | 8775(2) | 5363(1) | 4151(1) | 34(1) |
| O(4h) | 1828(2) | 4631(1) | 2824(1) | 35(1) |
| 215 K | | | | |
| Ca(1) | 5406(1) | 4106(1) | 3669(1) | 15(1) |
| N(1) | 5999(2) | 3729(1) | 1687(1) | 19(1) |
| N(2) | 4264(2) | 7337(1) | 4068(1) | 17(1) |
| O(1a) | 6639(2) | 4846(1) | 2168(1) | 26(1) |
| O(1b) | 5241(2) | 2695(1) | 2114(1) | 26(1) |
| O(1c) | 6130(2) | 3658(1) | 846(1) | 32(1) |
| O(2a) | 4196(2) | 6211(1) | 4588(1) | 22(1) |
| O(2b) | 4777(1) | 7142(1) | 3271(1) | 22(1) |
| O(2c) | 3830(2) | 8557(1) | 4354(1) | 28(1) |
| O(2h) | 8217(2) | 2237(1) | 3966(1) | 28(1) |
| O(3h) | 3125(2) | 1959(1) | 3839(1) | 42(1) |
| O(1h) | 8800(2) | 5375(1) | 4151(1) | 24(1) |
| O(4h) | 1828(2) | 4645(1) | 2821(1) | 25(1) |
| H(1a) | 8880(40) | 6249(19) | 4004(17) | 70(7) |
| H(1b) | 9390(80) | 5230(60) | 4702(19) | 172(19) |
| H(2a) | 8220(40) | 1860(30) | 4493(13) | 67(7) |
| H(2b) | 8150(30) | 1522(19) | 3604(13) | 49(6) |
| H(3a) | 3600(40) | 1310(30) | 4220(17) | 84(9) |
| H(3b) | 1790(30) | 2060(50) | 3820(30) | 171(18) |
| H(4a) | 1260(30) | 3976(19) | 2500(13) | 45(5) |
| H(4b) | 1740(60) | 5430(30) | 2550(20) | 114(12) |
| 100 K | | | | |
| Ca | 10834(1) | 4087(1) | 6333(1) | 7(1) |
| N(1) | 12114(1) | 3695(1) | 8306(1) | 9(1) |
| O(1a) | 12192(1) | 4842(1) | 7847(1) | 14(1) |
| O(1b) | 11481(1) | 2694(1) | 7875(1) | 12(1) |
| O(1c) | 12645(1) | 3555(1) | 9147(1) | 13(1) |
| N(2) | 10124(1) | 7359(1) | 5954(1) | 8(1) |
| O(2a) | 9859(1) | 6225(1) | 5423(1) | 10(1) |
| O(2b) | 10759(1) | 7165(1) | 6764(1) | 11(1) |
| O(2c) | 9761(1) | 8581(1) | 5662(1) | 13(1) |
| O(3h) | 12048(1) | 2256(1) | 6034(1) | 14(1) |
| O(2h) | 9614(1) | 1908(1) | 6156(1) | 14(1) |
| O(4h) | 12359(1) | 5352(1) | 5871(1) | 10(1) |
| O(1h) | 9453(1) | 4644(1) | 7167(1) | 11(1) |
| H(1a) | 8850(15) | 4964(18) | 6882(12) | 35(4) |
| H(1b) | 9342(14) | 3992(19) | 7494(12) | 31(4) |
| H(2a) | 8961(15) | 2013(19) | 6077(12) | 44(5) |
| H(2b) | 9680(13) | 1250(19) | 5765(12) | 31(4) |
| H(3a) | 12272(13) | 1564(19) | 6411(12) | 32(4) |
| H(3b) | 11929(15) | 1920(20) | 5544(14) | 43(5) |
| H(4a) | 12943(15) | 5152(18) | 6250(12) | 38(5) |
| H(4b) | 12390(13) | 6220(20) | 5909(11) | 28(4) |
| Ca′ | 5916(1) | 4130(1) | 6333(1) | 7(1) |
| N(1′) | 7190(1) | 3796(1) | 8323(1) | 9(1) |
| O(1a′) | 7277(1) | 4915(1) | 7831(1) | 12(1) |

Table 4 (*Continued*)

| | *x* | *y* | *z* | *U*(eq) |
|---|---|---|---|---|
| O(1b′) | 6611(1) | 2745(1) | 7902(1) | 13(1) |
| O(1c′) | 7659(1) | 3753(1) | 9178(1) | 15(1) |
| N(2′) | 5098(1) | 7349(1) | 5913(1) | 8(1) |
| O(2a′) | 4808(1) | 6215(1) | 5391(1) | 10(1) |
| O(2b′) | 5773(1) | 7158(1) | 6708(1) | 10(1) |
| O(2c′) | 4717(1) | 8569(1) | 5632(1) | 12(1) |
| O(3h′) | 7235(1) | 2284(1) | 6011(1) | 11(1) |
| O(2h′) | 4860(1) | 1872(1) | 6268(1) | 16(1) |
| O(4h′) | 7343(1) | 5428(1) | 5832(1) | 11(1) |
| O(1h′) | 4504(1) | 4668(1) | 7165(1) | 11(1) |
| H(1a′) | 4609(13) | 5333(19) | 7487(11) | 33(5) |
| H(1b′) | 4377(15) | 3950(20) | 7477(12) | 37(5) |
| H(2a′) | 4951(15) | 1390(20) | 6704(14) | 51(6) |
| H(2b′) | 4758(15) | 1260(20) | 5838(14) | 48(5) |
| H(3a′) | 7289(14) | 1560(20) | 6403(12) | 34(4) |
| H(3b′) | 6966(14) | 1947(18) | 5508(12) | 29(4) |
| H(4a′) | 7427(12) | 5200(17) | 5294(13) | 36(4) |
| H(4b′) | 7439(13) | 6270(20) | 5913(11) | 30(4) |

*U*(eq) is defined as one third of the trace of the orthogonalized $U_{ij}$ tensor.

Table 5
Comparison of bond lengths (Å) for $[Ca(H_2O)_4](NO_3)_2$ at 293, 215 and 100 K

| | 293 K | 215 K | 100 K | |
|---|---|---|---|---|
| | | | 1st molecule | 2nd molecule |
| Ca(1)–O(1h) | 2.4287(18) | 2.4258(17) | 2.4203(10) | 2.4468(10) |
| Ca(1)–O(2h) | 2.4436(16) | 2.4414(15) | 2.4706(12) | 2.4293(13) |
| Ca(1)–O(3h) | 2.4621(16) | 2.4575(15) | 2.3693(11) | 2.4843(11) |
| Ca(1)–O(4h) | 2.4396(18) | 2.4347(18) | 2.4664(10) | 2.4092(10) |
| Ca(1)–O(1a) | 2.4964(12) | 2.4903(12) | 2.4997(10) | 2.4926(10) |
| Ca(1)–O(1b) | 2.5839(13) | 2.5734(12) | 2.4863(12) | 2.5297(11) |
| Ca(1)–O(2a) | 2.5212(13) | 2.5138(12) | 2.5101(11) | 2.4726(11) |
| Ca(1)–O(2a)[a] | 2.5155(13) | 2.5053(12) | 2.5346(10) | 2.5676(10) |
| Ca(1)–O(2b) | 2.8400(18) | 2.8510(17) | 2.8848(17) | 2.8317(17) |
| Ca(1)–N(1) | 2.9592(14) | 2.9508(14) | 2.9317(12) | 2.9441(12) |
| Ca(1)–N(2) | 3.1114(18) | 3.1133(18) | 3.1186(18) | 3.1129(18) |
| Ca(1)–Ca(1)[a] | 4.2795(14) | 4.2672(14) | 4.2498(12) | 4.2738(12) |
| N(1)–O(1a) | 1.2634(15) | 1.2660(14) | 1.2634(12) | 1.2731(12) |
| N(1)–O(1b) | 1.2527(15) | 1.2568(14) | 1.2590(12) | 1.2561(12) |
| N(1)–O(1a) | 1.2261(14) | 1.2282(14) | 1.2406(11) | 1.2365(12) |
| N(2)–O(2a) | 1.2742(14) | 1.2775(13) | 1.2851(12) | 1.2807(12) |
| N(2)–O(2b) | 1.2453(14) | 1.2487(14) | 1.2510(11) | 1.2529(11) |
| N(2)–O(2c) | 1.2285(15) | 1.2324(14) | 1.2347(12) | 1.2356(12) |

[a] $-x+2, -y+1, -z+1$ for the first molecule at 100 K and $2-x+1, -y+1, -z+1$ for remain molecules.

belonging to nitrate anions (three in the same asymmetric unit and two symmetry related) with mean $Ca^{2+}$–O distance 2.591 Å. Note that distance $Ca^{2+}$–O(2b) has value 2.840 Å and is significantly greater than other. Oxygen atom O(2a) is shared between two, related by centre of inversion, $Ca^{2+}$ cations with similar 2.516 and 2.521 Å distances and join two symmetry related parts, forming dimmer (see Fig. 4 drown in ORTEP [13,14]).

Detailed geometrical parameters of tetraaquacalcium nitrate(V) at room temperature, compared with appropriate parameters at temperatures 215 and 100 K, are listed in Table 4 (fractional coordination's and *U*(eq)) and Table 5 (selected bond lengths). This parameters are close to the reported earlier, for the structures determined at room temperature [1–3]. Comparison of the structure determined at 215 K and room temperature (see Tables 2 and 5) shows no significant differences. The interatomic distances (with exception of N–O distance in nitrate(V) group) and atoms displacements parameters are slightly decreasing, which is natural consequence of the temperature decreasing (Fig. 5).

As shown in Fig. 6 drown in ORTEP [13,14], repeating unit of the structure determined at 100 K contains two, original and primed $[Ca(H_2O)_4](NO_3)_2$ dimers. These dimmers can be brought near to overlap when one of them is translated by 1/2a. Table 6 lists the values of the differences in the atomic positions of "overlapped" fragments in the structure at 100 K. The resultant shifts of the atoms given in the last column have the greatest values for the water molecules oxygen atoms, O(2h) and O(3h). In consequence of these movements the centre of inversion located at geometrical centre of these dimmers, observed in the structure at 293 K and 215 K disappears and these two molecules became symmetrically independent. Cell volume is

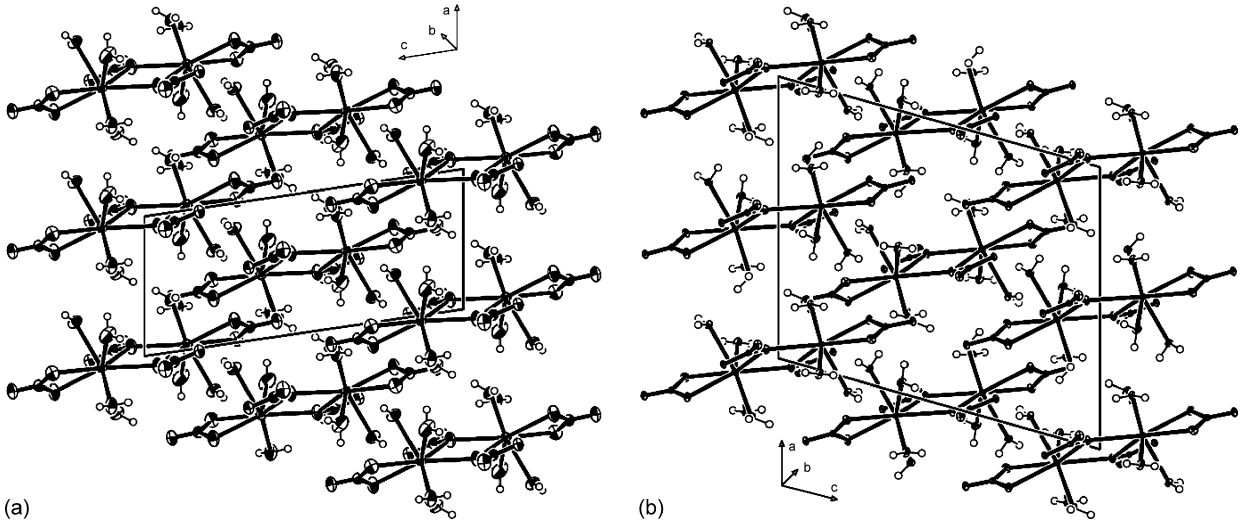


Fig. 5. Molecular packing of $[Ca(H_2O)_4](NO_3)_2$ at (a) 293 K and (b) 100 K.

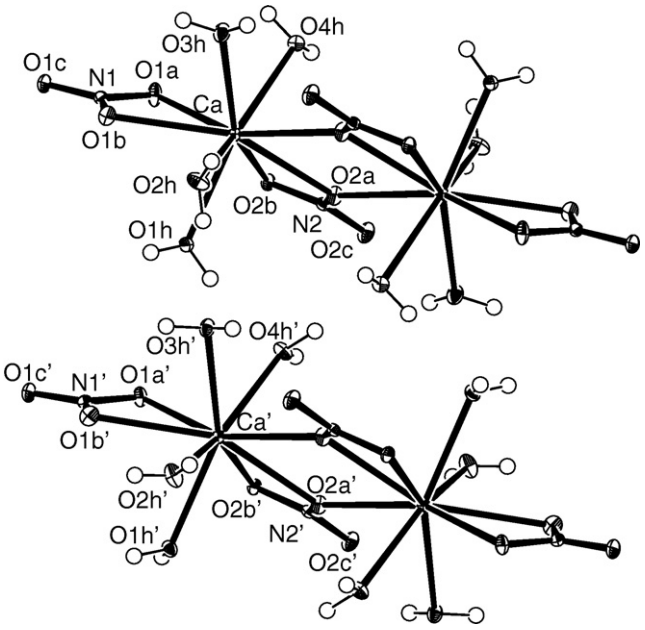


Fig. 6. ORTEP [13,14] projections of repeating fragment of the $[Ca(H_2O)_4](NO_3)_2$ at 100 K.

approximately doubled and $Z = 8$. It is interesting that the same space group symbol $P2_1/n$ can be assigned to the new lattice. Another consequences of the geometrical differences between original and primed dimers are changes in water molecules orientations. For example: hydrogen atom H 1a connected to the O 1h of the water molecule is turned to the O 4h′ oxygen atom in neighbouring primed molecule. These three atoms form hydrogen bond in which O 1h is a donor and O 4h′ is an acceptor of proton. Analogue hydrogen atom H 1a′ is directed to O 2h related by the symmetry operation $[-x+3/2, y+1/2, -z+3/2]$ and forming O 1h′–H 1a′···O 2h hydrogen bond. The H 1b and H 1b′ atoms connected to O 1h and O 1h′ atoms, respectively, have approximately the same orientation and form hydrogen bonds to the related by the symmetry operation $[-x+3/2, y-1/2, -z+3/2]$ O 2b′ and O 2b atoms, respectively (see Figs. 6 and 7). Geometrical details of these and other hydrogen bonds observed in the crystal structures determined at 293, 215 and 100 K are listed in Table 7. Fig. 7 shows the differences in the hydrogen bonds net in the structure determined at 293 and 100 K.

Table 6
Values of differences in atomic positions in the structure of $[Ca(H_2O)_4](NO_3)_2$ at 100 K

| | $\Delta x$ | $\Delta x/\sigma x$ | $\Delta y$ | $\Delta y/\sigma y$ | $\Delta z$ | $\Delta z/\sigma z$ | Shift (Å) |
|---|---|---|---|---|---|---|---|
| Ca/Ca′ | 0.00812 | 406.00 | 0.00425 | 212.50 | 0.00005 | 5.00 | 0.10796 |
| N(1)/N(1′) | 0.00756 | 108.00 | 0.01005 | 111.67 | 0.00167 | 27.83 | 0.13113 |
| O(1a)/O(1a′) | 0.00849 | 141.50 | 0.00730 | 91.25 | −0.00159 | −31.80 | 0.12951 |
| O(1b)/O(1b′) | 0.01301 | 216.83 | 0.00510 | 63.75 | 0.00271 | 54.20 | 0.16769 |
| O(1c)/O(1c′) | 0.00140 | 23.33 | 0.01975 | 219.44 | 0.00318 | 63.60 | 0.18632 |
| N(2)/N(2′) | −0.00262 | −37.43 | −0.00106 | −11.78 | −0.00412 | −68.67 | 0.06555 |
| O(2a)/O(2a′) | −0.00506 | −84.33 | −0.00096 | −12.00 | −0.00325 | −65.00 | 0.07417 |
| O(2b)/O(2b′) | 0.00133 | 22.17 | −0.00063 | −7.88 | −0.00562 | −112.40 | 0.08675 |
| O(3c)/O(3c′) | −0.00439 | −73.17 | −0.00123 | −15.37 | −0.00303 | −60.60 | 0.06655 |
| O(1h)/O(1h′) | 0.00509 | 84.83 | 0.00241 | 26.78 | −0.00016 | −3.20 | 0.06728 |
| O(2h)/O(2h′) | 0.02455 | 350.71 | −0.00355 | −39.44 | 0.01114 | 185.67 | 0.32767 |
| O(3h)/O(3h′) | 0.01876 | 268.00 | 0.00273 | 30.33 | −0.00237 | −39.50 | 0.24155 |
| O(4h)/O(4h′) | −0.00161 | −26.83 | 0.00758 | 84.22 | −0.00389 | −77.80 | 0.09027 |

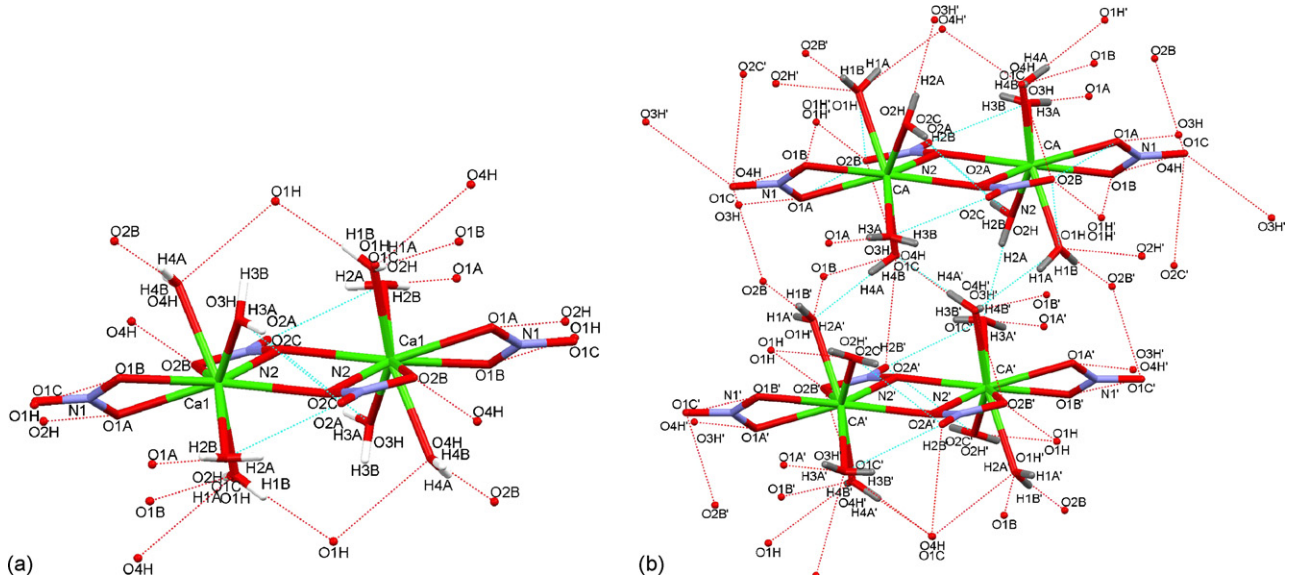


Fig. 7. MERCURY plot of the hydrogen bond net in crystal structure of the $[Ca(H_2O)_4](NO_3)_2$ at (a) 293 K and (b) 100 K.

Table 7
Hydrogen bonds with distances D···A < 3.000 Å and angles DHA > 110°

| D–H | *d*(D–H) | *d*(H···A) | <DHA | *d*(D···A) | A |
|---|---|---|---|---|---|
| 293 K | | | | | |
| O 1h–H 1a | 0.830 | 2.214 | 161.73 | 3.014 | O 1c [−*x*+3/2, *y*+1/2, −*z*+1/2] |
| O 1h–H 1a | 0.830 | 2.249 | 139.85 | 2.933 | O 1b [−*x*+3/2, *y*+1/2, −*z*+1/2] |
| O 1h–H 1a | 0.830 | 2.502 | 168.85 | 3.320 | N1 [−*x*+3/2, *y*+1/2, −*z*+1/2] |
| O 1h–H 1b | 0.826 | 1.964 | 171.87 | 2.784 | O 1h [−*x*+2, −*y*+1, −*z*+1] |
| O 2h–H 2a | 0.838 | 2.253 | 147.51 | 2.994 | O 2c [−*x*+1, −*y*+1, −*z*+1] |
| O 2h–H 2a | 0.838 | 2.563 | 130.33 | 3.171 | O 1c [*x*+1/2, −*y*+1/2, *z*+1/2] |
| O 2h–H 2b | 0.837 | 1.920 | 172.95 | 2.753 | O 1a [−*x*+3/2, *y* − 1/2, −*z*+1/2] |
| O 2h–H 2b | 0.837 | 2.663 | 149.86 | 3.413 | N1 [−*x*+3/2, *y* − 1/2, −*z*+1/2] |
| O 3h–H 3a | 0.832 | 2.448 | 128.20 | 3.034 | O 2c [−*x*+1, −*y*+1, −*z*+1] |
| O 3h–H 3a | 0.832 | 2.541 | 141.17 | 3.232 | O 2c [*x*, *y* − 1, *z*] |
| O 3h–H 3b | 0.849 | 2.297 | 169.69 | 3.136 | O 2h [*x* − 1, *y*, *z*] |
| O 4h–H 4a | 0.791 | 2.109 | 169.16 | 2.890 | O 2b [−*x*+1/2, *y* − 1/2, −*z*+1/2] |
| O 4h–H 4b | 0.806 | 2.418 | 142.00 | 3.094 | O 1b [−*x*+1/2, *y*+1/2, −*z*+1/2] |
| O 4h–H 4b | 0.806 | 2.575 | 141.37 | 3.244 | O 3h [−*x*+1/2, *y*+1/2, −*z*+1/2] |
| 215 K | | | | | |
| O 1h–H 1a | 0.829 | 2.214 | 158.89 | 3.003 | O 1c [−*x*+3/2, *y*+1/2, −*z*+1/2] |
| O 1h–H 1a | 0.829 | 2.214 | 142.16 | 2.914 | O 1b [−*x*+3/2, *y*+1/2, −*z*+1/2] |
| O 1h–H 1a | 0.829 | 2.483 | 171.15 | 3.305 | N1 [−*x*+3/2, *y*+1/2, −*z*+1/2] |
| O 1h–H 1b | 0.836 | 1.944 | 166.93 | 2.765 | O 1h [−*x*+2, −*y*+1, −*z*+1] |
| O 2h–H 2a | 0.833 | 2.271 | 143.78 | 2.984 | O 2c [−*x*+1, −*y*+1, −*z*+1] |
| O 2h–H 2a | 0.833 | 2.508 | 133.98 | 3.144 | O 1c [*x*+1/2, −*y*+1/2, *z*+1/2] |
| O 2h–H 2b | 0.834 | 1.909 | 173.24 | 2.739 | O 1a [−*x*+3/2, *y* − 1/2, −*z*+1/2] |
| O 2h–H 2b | 0.834 | 2.655 | 149.43 | 3.399 | N1 [−*x*+3/2, *y* − 1/2, −*z*+1/2] |
| O 3h–H 3a | 0.835 | 2.418 | 130.66 | 3.029 | O 2c [−*x*+1, −*y*+1, −*z*+1] |
| O 3h–H 3a | 0.835 | 2.526 | 140.47 | 3.215 | O 2c [*x*, *y* − 1, *z*] |
| O 3h–H 3b | 0.837 | 2.271 | 172.24 | 3.102 | O 2h [*x* − 1, *y*, *z*] |
| O 4h–H 4a | 0.815 | 2.064 | 172.44 | 2.874 | O 2b [−*x*+1/2, *y* − 1/2, −*z*+1/2] |
| O 4h–H 4b | 0.816 | 2.495 | 129.56 | 3.080 | O 1b [−*x*+1/2, *y*+1/2, −*z*+1/2] |
| O 4h–H 4b | 0.816 | 2.450 | 152.55 | 3.196 | O 3h [−*x*+1/2, *y*+1/2, −*z*+1/2] |
| 100 K | | | | | |
| O 1h–H 1a | 0.807 | 2.122 | 164.05 | 2.907 | O 4h′ |
| O 1h–H 1a | 0.807 | 2.639 | 119.07 | 3.112 | O 1b′ [−*x*+3/2, *y*+1/2, −*z*+3/2] |
| O 1h–H 1b | 0.800 | 2.071 | 172.36 | 2.866 | O 2b′ [−*x*+3/2, *y* − 1/2, −*z*+3/2] |
| O 2h–H 2a | 0.793 | 2.134 | 174.34 | 2.924 | O 3h′ |
| O 2h–H 2b | 0.851 | 2.391 | 130.87 | 3.017 | O 2c [−*x*+2, −*y*+1, −*z*+1] |
| O 2h–H 2b | 0.851 | 2.443 | 139.25 | 3.137 | O 2c [*x*, *y*−1, *z*] |
| O 3h–H 3a | 0.837 | 1.926 | 173.35 | 2.759 | O 1a [−*x*+5/2, *y* − 1/2, −*z*+3/2] |
| O 3h–H 3b | 0.761 | 2.398 | 133.22 | 2.971 | O 2c [−*x*+2, −*y*+1, −*z*+1] |
| O 3h–H 3b | 0.761 | 2.496 | 147.59 | 3.165 | O 1c′ [*x*+1/2, −*y*+1/2, *z* − 1/2] |
| O 4h–H 4a | 0.808 | 2.086 | 176.33 | 2.892 | O 1h′ [*x*+1, *y*, *z*] |
| O 4h–H 4b | 0.796 | 2.370 | 128.72 | 2.934 | O 1b [−*x*+5/2, *y*+1/2, −*z*+3/2] |
| O4h-H4b | 0.796 | 2.129 | 173.59 | 2.921 | O 1c [−*x*+5/2, *y*+1/2, −*z*+3/2] |
| O 1h′–H 1a′ | 0.759 | 2.437 | 161.06 | 3.164 | O 2h [−*x*+3/2, *y*+1/2, −*z*+3/2] |
| O 1h′–H 1a′ | 0.759 | 2.523 | 123.96 | 3.013 | O 1b [−*x*+3/2, *y*+1/2, −*z*+3/2] |
| O 1h′–H 1b′ | 0.839 | 2.007 | 174.02 | 2.843 | O 2b [−*x*+3/2, *y* − 1/2, −*z*+3/2] |
| O 2h′–H 2a′ | 0.759 | 2.279 | 164.70 | 3.017 | O 1h [−*x*+3/2, *y* − 1/2, −*z*+3/2] |
| O 2h′–H 2b′ | 0.831 | 2.429 | 127.77 | 3.011 | O 2c′ [−*x*+1, −*y*+1, −*z*+1] |
| O 2h′–H 2b′ | 0.831 | 2.468 | 139.43 | 3.146 | O 2c′ [*x*, *y* − 1, *z*] |
| O 3h′–H 3a′ | 0.867 | 1.867 | 166.24 | 2.717 | O 1a′ [−*x*+3/2, *y* − 1/2, −*z*+3/2] |
| O 3h′–H 3b′ | 0.787 | 2.347 | 145.04 | 3.026 | O 2c′ [−*x*+1, −*y*+1, −*z*+1] |
| O 3h′–H 3b′ | 0.787 | 2.420 | 134.29 | 3.023 | O 1c [*x*−1/2, −*y*+1/2, *z* − 1/2] |
| O 4h′–H 4a′ | 0.852 | 1.875 | 178.20 | 2.726 | O 4h [−*x*+2, −*y*+1, −*z*+1] |
| O 4h′–H 4b′ | 0.783 | 2.264 | 136.63 | 2.884 | O 1b′ [−*x*+3/2, *y*+1/2, −*z*+3/2] |
| O 4h′–H 4b′ | 0.783 | 2.267 | 165.49 | 3.032 | O 1c′ [−*x*+3/2, *y*+1/2, −*z*+3/2] |

### *3.3. Neutron scattering examinations*

The neutron diffraction patterns (NPD) for polycrystalline $[Ca(H_2O)_4](NO_3)_2$, registered during the sample heating up at five selected temperatures of measurement, are shown in Fig. 8 for two scattering angles: $2\theta = 69.10°$ and $61.25°$. We cannot see any important differences between the NPD patterns obtained for all three crystalline phases. It means that crystal structure of $[Ca(H_2O)_4](NO_3)_2$ does not change (or the changes are very small) after the phase transitions, at least from the point of view

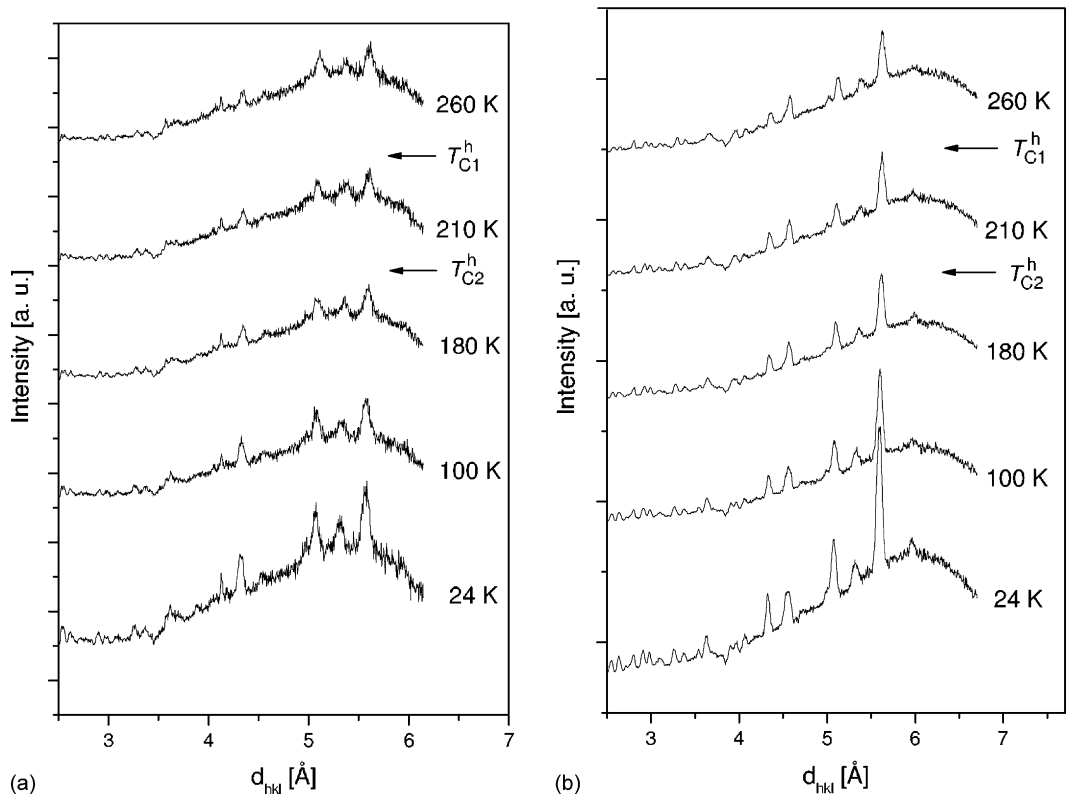


Fig. 8. The NPD patterns of $[Ca(H_2O)_4](NO_3)_2$ registered on heating the sample for seven chosen temperatures of measurement: (a) at scattering angle $2\theta = 69.10^\circ$ (with collimator) and (b) at mean scattering angle $2\theta = 61.25^\circ$.

of neutron diffraction method. As was stated above from single crystal measurements the change of the crystal structure in the $T_{C2}$ is very small. It is mainly connected with changes in water molecule orientations. This aspect cannot be seen and investigated by means of neutron diffraction mainly due to high incoherent cross-section scattering for hydrogen atoms. That is why neutron powder diffraction method is insensitive for water molecules orientation and one can not see doubled reflection in the diffraction pattern below $T_{C2}$. This conclusion is compatible with the results obtained by us from X-ray single crystal measurements.

## 4. Conclusions

1. The DSC measurements of $[Ca(H_2O)_4](NO_3)_2$ performed in the temperature range of 95–298 K allowed two phase transitions to be detect. The temperature of these phase transitions, obtained by extrapolation of the corresponding $T_{peak}^{h}$ and $T_{peak}^{c}$ values obtained at different scanning rate to the zero scanning rate, amount to: $T_{C1}^{h} = 243.7\,K$, $T_{C2}^{h} = 203.3\,K$ (on heating) and $T_{C1}^{c} = 222.0\,K$, $T_{C2}^{c} = 201.5\,K$ (on cooling). The value of $\Delta S_1 = 5.8\,J\,mol^{-1}\,K^{-1}$ (Rln2) indicates for some kind of orientational dynamical disorder of in the high temperature phase.
2. The diffraction pattern at 293 K is nearly exactly the same as at 215 K, what implies that phase transition at $T_{C1}$ has not structural character. However, there are some characteristic changes at the X-ray diffraction patterns at 100 K, what implies that phase transition at $T_{C2}$ is connected with a change of the crystal structure. Namely, at 100 K the unit cell is doubled and atom positions show scant but statistically significant differences between 100 and 215 K. The space group ($P2_1/n$; No. 14) is the same for high, intermediate and low temperatures phases. However, changes of water molecule orientations and changes in the net of hydrogen bonds are clearly visible.

## Acknowledgements

Our thanks are due to Professor S. Wróbel from the Faculty of Physics, Astronomy and Applied Computer Science of the Jagiellonian University and to Dr. I. Natkaniec from Frank Laboratory of Neutron Physics JINR, Dubna in Russia and from H. Niewodniczański Institute of Nuclear Physics, Polish Academy of Sciences, Kraków, Poland, for enabling us to perform DSC and neutron diffraction powder measurements, respectively.

## References

[1] A. Leclaire, I.C. Monier, C. R. Acad. Sci. Paris 271 (1970) 1555–1557.
[2] A. Leclaire, I.C. Monier, Acta Crystallogr. B 33 (1977) 1861–1866.
[3] B. Ribar, V. Divjaković, Acta Crystallogr. B 29 (1973) 1546–1548.
[4] E. Mikuli, A. Migdał-Mikuli, S. Wróbel, B. Grad, Z. Naturforsch. 54A (1999) 595–598.
[5] J.M. Janik, E. Mikuli, A. Migdał-Mikuli, M. Rachwalska, T. Stanek, J.A. Janik, K. Otnes, I. Svare, Phys. Scripta 28 (1983) 569–572.
[6] B. Borzęcka-Prokop, E. Kapturkiewicz, A. Wesełucha-Birczyńska, S.A. Hodorowicz, Crys. Res. Technol. 25 (1990) 1311–1320.

[7] A. Migdał-Mikuli, J. Hetmańczyk, Ł. Hetmańczyk, J. Therm. Anal. Calorim., in press.
[8] E. Mikuli, A. Migdał-Mikuli, S. Wróbel, Z. Naturforsh. 54A (1999) 225–228.
[9] Z. Otwinowski, W. Minor, in: C.W. Carter Jr., R.M. Sweet (Eds.), Processing of X-ray Diffraction Data Collected in Oscillation Mode, Methods in Enzymology: Macromolecular Crystallography, Part A, vol. 276, Academic Press, 1997, pp. 307–326.
[10] A. Altomare, G. Cascarano, C. Giacovazzo, A. Guagliardi, J. Appl. Crystallogr. 26 (1993) 343–350.
[11] G.M. Sheldrick, SHELXL-97 Programs for Crystal Structure Analysis (Release 97-2), Institut für Anorganische Chemie der Universität, Tammanstrasse 4, D-3400 Göttingen, Germany, 1998.
[12] I. Natkaniec, S.I. Bragin, J. Brańkowski, J. Mayer, in: Proceedings ICANS XII Meeting, Abington 1993. RAL Report 94-025, vol. I, 1994, pp. 89–96.
[13] L.J. Farrugia, J. Appl. Crystallogr. 30 (1977) 565.
[14] M.N. Burnett, C.K. Johnson, *ORTEP-III*, Report ORNL-6895. Oak Ridge National Laboratory, Oak Ridge, Tennessee, 1996.